

Table of Contents

Figure S1. Production rhGNS using pCI-neo vector.	S-2
Figure S2. More characterization of purified rhGNS.	S-2
Figure S3. Production and characterization of rhGNS using popvec vector.	S-3
Table S1. PCR and Sequence primers	S-4
Table S2. Plasmid information	S-4
Table S3. Purification of rhGNS produced in CHO cells transfected with TCB469.	S-4
Table S4. LC/MS/MS analysis of trypsin digested rhGNS further confirmed the identity of rhGNS.	S-5
Table S5. Quantification the purity of rhGNS purified from TCB469 B2 using ImageJ.	S-5
Table S6. Purification of rhGNS produced in TCB616 C2	S-5
Table S7. LC/MS/MS analysis of trypsin digested rhGNS further confirmed the identity of rhGNS purified from TCB616 C2	S-6 - 9
Supplemental Methods	S-10 - 12

Supplemental Figures

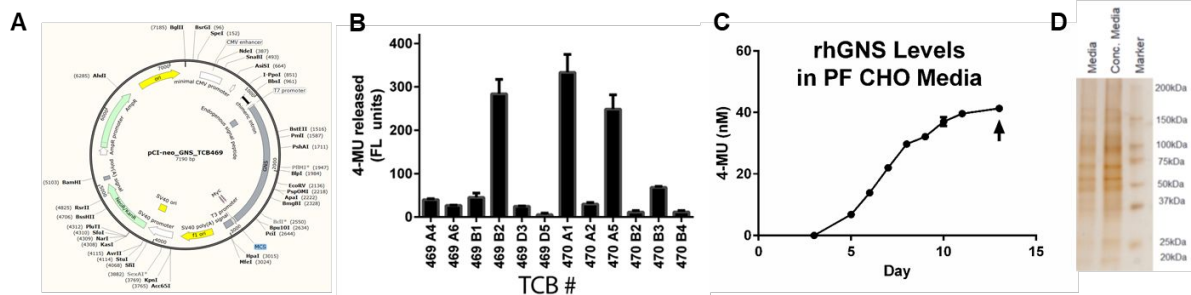


Figure S1. Production rhGNS using pCI-neo vector. A) rhGNS expression plasmid. B) rhGNS high expression clone selection. C-D) Monitor of rhGNS secretion via GNS activity (C) and SDS-PAGE (D).

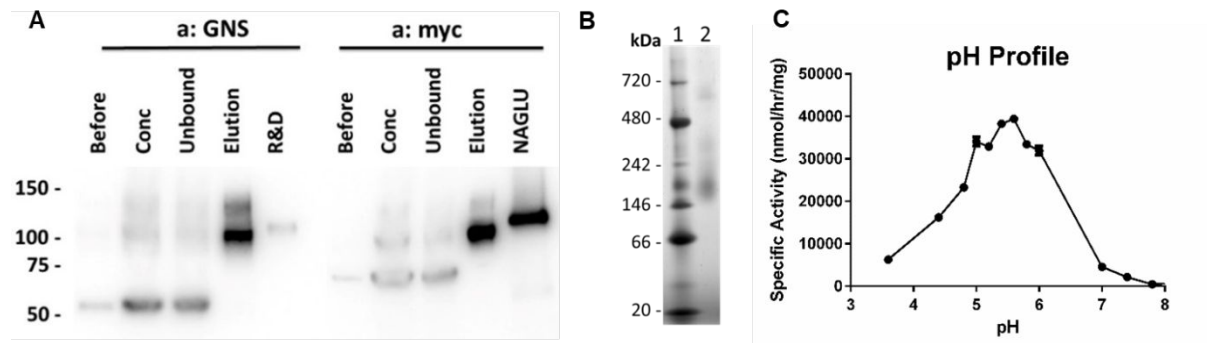


Figure S2. A) Identification of rhGNS using antibodies against GNS and myc. B) Native PAGE of rhGNS. Purified rhGNS was resolved in a non-denaturing Tris/Bis gel by electrophoresis, exhibiting an estimated molecular weight of 160-200 kDa, suggesting that it forms either a homodimer or trimer conformation. C) pH profile of rhGNS using the sulfatase assay. Both the commercially available and our own product demonstrated a pH optimum of approximately 5.6 against the substrate PNCS with overlapping pH profiles

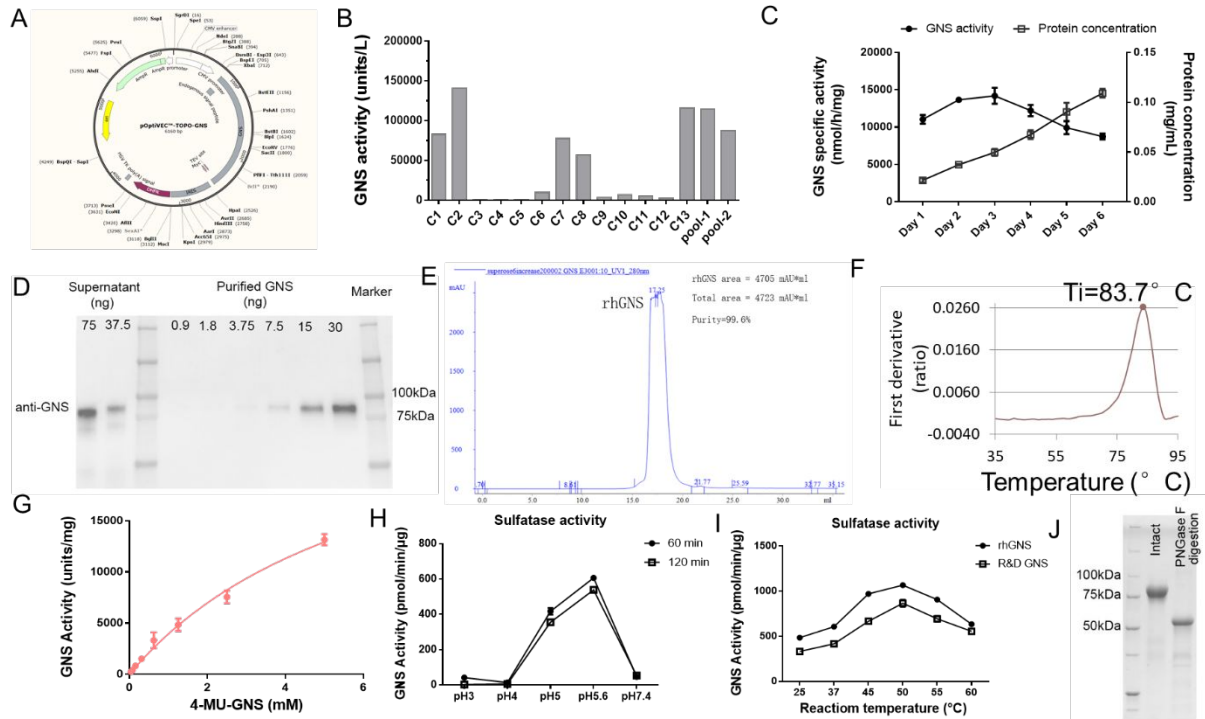


Figure S3. Production and characterization of rhGNS using popvec vector. A) rhGNS expression plasmid TCB616. B) rhGNS high expression clone selection. C) Monitor of rhGNS secretion via GNS activity. D) Quantified the percentage of rhGNS in total secreted proteins via western blot. E) The purity of purified rhGNS detected by size exclusion chromatography. F) The inflection temperature of rhGNS is 83.7°C. G) Michaelis-Menten kinetics curve of rhGNS purified from TCB616 C2. The calculated K_m was 6.0 ± 1.2 mM, and the estimated k_{cat} was determined to be 3.0×10^4 units/mg. H) Sulfatase activity detected the pH profile of rhGNS. I) Sulfatase activity detected the temperature profile of purified rhGNS and the commercial R&D GNS. J) SDS-PAGE of purified rhGNS treated by glycosidase PNGase F.

Supplemental Tables

Table S1. PCR and Sequence primers

Primer #	Sequence
1	CCAAGCATCTGCTGGGGGGTAAAACTTGTATTTCCAGGGCGGCGGTTCCGGGGGGGGGG
2	CCCCCCCCCGGAACCGCCGCCCTGGAAATACAAGTTTTACCCCCCAGCAGATGCTTGG
3	CACCATGAGACTGCTGCCCCTGGCTC
4	GCCGCTTATTATTACAGGTCCTCTTC
5	CGCAAATGGGCGGTAGGCGTG
6	GGCACCTATTGGTCTTACTGACATCC
7	CTGAAGAAAACAAAGGCCCTGATCGG
8	CTGGTATGCCCTGGAGAAGAATAGC
9	CAAATTCATCCATCCAGTTCCTGGAC
10	CCATCCTGGACATTGCAGGTTACG
11	CATTGCCAAGACTATCGACCCAG
12	GTACTCATTCTTGCAGAAGACCC
13	CTTCAGTGGCGTCTACAAAGC
14	AGTGCCACCAAGCAGAACTC

Table S2. Plasmid made in this study

Plasmid number	Vector
TCB469	pCl-neo
TCB470	pCl-neo
TCB616	pOptiVEC™-TOPO

Table S3. Purification of rhGNS produced in CHO cells transfected with TCB469.

Step	Volume (mL)	Total Protein (mg)	Total Units (nmol/hr)	Specific Activity (nmol/hr/mg)	Fold-enrichment	% Yield
Before	725	118	3993.8	33.7	1	
Conc.	100	114	25943	226.6	6.7	100%
Unbound	100	113	11669	94.8	2.8	45%
Elution	0.2	0.16	2086	13400	397.4	8%

Note: 1 unit = 1 nmol converted substrate per h at 37 °C. The substrate is 4-methylumbelliferyl *N*-acetylglucosamine-6-sulfate.

Table S4. LC/MS/MS analysis of trypsin digested rhGNS further confirmed the identity of rhGNS purified from TCB469 B2.

Description	Abundance	Normalized to GNS Abundance (%)	Coverage	# AAs	MW (kDa)
glucosamine (N-acetyl)-6-sulfatase (GNS)	5.48E10	100	49.64	552	62.1
Histone H4 OS=Homo sapiens	2.12E9	4	51.46	103	11.4
Isoform 3 of T-complex protein 1 subunit eta	2.80E9	5	30.06	499	54.8

Note: analysis of rhGNS from myc affinity purification by LC/MS/MS analysis determined two major contaminant proteins are Histone H4 and Isoform 3 of T-complex protein 1 subunit eta (CCT7).

Table S5. Quantification the purity of rhGNS purified from TCB469 B2 using ImageJ.

	Total area	80 kDa band	Purity (%)
2.5 µg	1.33E+05	5.13E+04	38.4
	1.33E+05	5.59E+04	41.9
5 µg	1.64E+05	8.92E+04	54.2
	1.64E+05	9.77E+04	59.4
Average			48.5

Table S6. Purification of rhGNS produced in TCB616 C2.

Step	Volume (ml)	Total Protein (mg)	Total Units (nmol/hr)	Specific Activity (nmol/hr/mg)	Fold-enrichment	% Yield	% Yield (Normalized)
Before	800	93	611438	6570	1		
Conc.	40	78	552750	7045	1.1	100%	
Load	10	21	146906	7045	1.1	27%	100%
Unbound	12	13	83529	6202	0.9	15%	62%
Elution	4	3	2086	38989	5.9	3.8%*	14.3%*

*Yield of 3.8% is calculated from 78 mg of total protein: we only took 21 mg to load onto the myc-agarose due to its binding capacity. The normalized yield to 21 mg is 14.3%.

Table S7. LC/MS/MS analysis of trypsin digested rhGNS further confirmed the identity of rhGNS purified from TCB616 C2.

Description	Abundance	Normalized to GNS Abundance (%)	MW (kDa)	Calc pI
N-acetylglucosamine-6-sulfatase OS=Homo sapiens OX=9606 GN=GNS PE=1 SV=3	6.90E+09	100.000	62.00	8.31
Endoplasmic reticulum chaperone BiP OS=Cricetulus griseus OX=10029 GN=HSPA5 PE=1 SV=1	2.18E+07	0.316	72.30	5.16
Transducin-like enhancer protein 1 OS=Homo sapiens OX=9606 GN=TLE1 PE=1 SV=2	1.68E+07	0.243	83.10	7.24
Galectin-3-binding protein OS=Cricetulus griseus OX=10029 GN=CgPICR_011982 PE=4 SV=1	1.60E+07	0.233	63.8	5.19
Histone H4 OS=Cricetulus griseus OX=10029 GN=I79_012827 PE=3 SV=1	4.95E+06	0.072	28.4	11.03
N-acetylglucosamine-6-sulfatase OS=Cricetulus griseus OX=10029 GN=I79_019923 PE=3 SV=1	3.84E+06	0.056	53.7	6.87
Peptidyl-prolyl cis-trans isomerase OS=Cricetulus griseus OX=10029 GN=CgPICR_005246 PE=3 SV=1	3.06E+06	0.044	23.6	9.58
Cation-independent mannose-6-phosphate receptor OS=Cricetulus griseus OX=10029 GN=I79_009791 PE=4 SV=1	2.26E+06	0.033	186.5	5.41
Ubiquinone biosynthesis O-methyltransferase, mitochondrial OS=Homo sapiens OX=9606 GN=COQ3 PE=1 SV=3	2.15E+06	0.031	41	7.42
Histone H3.1t OS=Cricetulus griseus OX=10029 GN=I79_010126 PE=3 SV=1	1.99E+06	0.029	35.8	10.71
Annexin OS=Cricetulus griseus OX=10029 GN=I79_018648 PE=3 SV=1	1.66E+06	0.024	36	5.05
(Common contaminant protein)	1.62E+06	0.023	24.4	7.18
LGMN OS=Cricetulus griseus OX=10029 GN=CgPICR_012975 PE=1 SV=1	1.46E+06	0.021	49.6	6.55
Ferritin OS=Cricetulus griseus OX=10029 GN=CgPICR_006768 PE=3 SV=1	1.32E+06	0.019	21.5	6.16
Dermatopontin OS=Cricetulus griseus OX=10029 GN=I79_008827 PE=4 SV=1	1.09E+06	0.016	24	4.89
Histone H4 OS=Cricetulus griseus OX=10029 GN=I79_012828 PE=3 SV=1	1.09E+06	0.016	21.8	10.7
Annexin A2 OS=Homo sapiens OX=9606 GN=ANXA2 PE=1 SV=2	1.06E+06	0.015	38.6	7.75
Cathepsin B OS=Cricetulus griseus OX=10029 GN=I79_003681 PE=3 SV=1	1.05E+06	0.015	37.5	6.13
ATP-binding cassette sub-family A member 9 OS=Homo sapiens OX=9606 GN=ABCA9 PE=1 SV=1	1.02E+06	0.015	184.2	6.93
Protein disulfide-isomerase A4 OS=Cricetulus griseus OX=10029 GN=CgPICR_019838 PE=3 SV=1	8.81E+05	0.013	72.5	5.17
Protein disulfide-isomerase OS=Homo sapiens OX=9606 GN=P4HB PE=1 SV=3	8.64E+05	0.013	57.1	4.87
Metalloproteinase inhibitor 2 OS=Cricetulus griseus OX=10029 GN=I79_004761 PE=4 SV=1	8.38E+05	0.012	21.5	7.52
Peroxiredoxin-1 OS=Cricetulus griseus OX=10029 GN=I79_002954 PE=4 SV=1	8.03E+05	0.012	22.2	7.72
CTS2 OS=Cricetulus griseus OX=10029 GN=ctsz PE=2 SV=1	7.90E+05	0.011	34	7.58
Cathepsin L1 OS=Cricetulus griseus OX=10029 GN=I79_025440 PE=3 SV=1	7.15E+05	0.010	37.2	7.17
Galectin OS=Cricetulus griseus OX=10029 GN=I79_006244 PE=4 SV=1	6.16E+05	0.009	32.4	7.37
Procollagen C-endopeptidase enhancer 1 OS=Cricetulus griseus OX=10029 GN=H671_4g12064 PE=4 SV=1	5.81E+05	0.008	55.2	8.13

Peroxiredoxin-4 (Fragment) OS=Homo sapiens OX=9606 GN=PRDX4 PE=1 SV=1	4.90E+05	0.007	18.3	6.19
Carboxypeptidase OS=Cricetulus griseus OX=10029 GN=I79_006816 PE=3 SV=1	4.78E+05	0.007	54.2	6.11
Ribonuclease T2 OS=Cricetulus griseus OX=10029 GN=I79_018311 PE=3 SV=1	4.75E+05	0.007	29.5	6.73
Cation-independent mannose-6-phosphate receptor OS=Homo sapiens OX=9606 GN=IGF2R PE=1 SV=3	4.62E+05	0.007	274.2	5.94
Lysosomal Pro-X carboxypeptidase OS=Cricetulus griseus OX=10029 GN=CgPICR_008653 PE=4 SV=1	4.53E+05	0.007	55.4	6.65
Protein S100 OS=Cricetulus griseus OX=10029 GN=CgPICR_013596 PE=3 SV=1	4.50E+05	0.007	10	5.48
Calmodulin OS=Cricetulus griseus OX=10029 GN=I79_024941 PE=3 SV=1	4.09E+05	0.006	16.7	4.39
Amyloid-beta precursor protein (Fragment) OS=Homo sapiens OX=9606 GN=APP PE=1 SV=1	4.01E+05	0.006	55.1	4.82
Nidogen-1 OS=Cricetulus griseus OX=10029 GN=I79_015301 PE=4 SV=1	3.92E+05	0.006	79	4.88
Alpha-galactosidase OS=Cricetulus griseus OX=10029 GN=I79_016839 PE=3 SV=1	3.81E+05	0.006	47.2	7.84
N-acetylglucosamine-6-sulfatase (Fragment) OS=Homo sapiens OX=9606 GN=GNS PE=1 SV=8	3.76E+05	0.005	28.3	8.9
Transaldolase OS=Cricetulus griseus OX=10029 GN=H671_3g9883 PE=3 SV=1	3.65E+05	0.005	37.5	7.03
SPARC OS=Homo sapiens OX=9606 GN=SPARC PE=1 SV=1	3.43E+05	0.005	34.6	4.84
Protein disulfide-isomerase A3 OS=Homo sapiens OX=9606 GN=PDIA3 PE=1 SV=4	3.20E+05	0.005	56.7	6.35
Annexin OS=Cricetulus griseus OX=10029 GN=H671_3g10393 PE=3 SV=1	3.19E+05	0.005	38.8	7.02
Beta-hexosaminidase OS=Cricetulus griseus OX=10029 GN=I79_015800 PE=3 SV=1	3.08E+05	0.004	60.1	7.36
Tubulointerstitial nephritis antigen-like OS=Cricetulus griseus OX=10029 GN=I79_004150 PE=3 SV=1	2.99E+05	0.004	52.5	7.08
Glutathione S-transferase P OS=Cricetulus griseus OX=10029 GN=I79_018157 PE=4 SV=1	2.94E+05	0.004	25	8.12
Deoxyribonuclease-2-alpha OS=Cricetulus griseus OX=10029 GN=H671_3g9963 PE=4 SV=1	2.70E+05	0.004	40.4	7.55
Protein disulfide-isomerase A6 OS=Cricetulus griseus OX=10029 GN=I79_007616 PE=4 SV=1	2.23E+05	0.003	28.4	4.91
Calcium-dependent serine proteinase OS=Cricetulus griseus OX=10029 GN=I79_001431 PE=3 SV=1	2.17E+05	0.003	77.4	4.82
Aspartate aminotransferase OS=Cricetulus griseus OX=10029 GN=CgPICR_007832 PE=4 SV=1	2.11E+05	0.003	46.2	7.21
Basement membrane-specific heparan sulfate proteoglycan core protein OS=Cricetulus griseus OX=10029 GN=I79_010495 PE=4 SV=1	2.10E+05	0.003	333.9	6.87
Laminin subunit gamma-1 OS=Cricetulus griseus OX=10029 GN=I79_009544 PE=4 SV=1	2.01E+05	0.003	172	5.07
EZR OS=Cricetulus griseus OX=10029 GN=CgPICR_011481 PE=4 SV=1	2.01E+05	0.003	69.3	6.37
Metalloproteinase inhibitor 1 OS=Cricetulus griseus OX=10029 GN=CgPICR_020423 PE=4 SV=1	1.96E+05	0.003	22.4	8.47
AGA OS=Cricetulus griseus OX=10029 GN=CgPICR_008921 PE=4 SV=1	1.77E+05	0.003	37.2	7.46
Calreticulin OS=Cricetulus griseus OX=10029 GN=CgPICR_020604 PE=3 SV=1	1.73E+05	0.003	48.2	4.49

Nucleolin OS=Cricetulus griseus OX=10029 GN=I79_022400 PE=4 SV=1	1.59E+05	0.002	52.4	4.5
Collagen alpha-1(III) chain OS=Cricetulus griseus OX=10029 GN=I79_024950 PE=4 SV=1	1.46E+05	0.002	114.9	4.94
Alpha-actinin-4 OS=Homo sapiens OX=9606 GN=ACTN4 PE=1 SV=2	1.38E+05	0.002	59.5	4.94
Sulfated glycoprotein 1 OS=Cricetulus griseus OX=10029 GN=I79_017410 PE=4 SV=1	1.27E+05	0.002	27.4	5.49
Procollagen-lysine,2-oxoglutarate 5-dioxygenase 1 OS=Cricetulus griseus OX=10029 GN=I79_023615 PE=4 SV=1	1.25E+05	0.002	75.9	6.2
Peptidyl-prolyl cis-trans isomerase-like 1 OS=Homo sapiens OX=9606 GN=PPIL1 PE=1 SV=1	1.20E+05	0.002	18.2	7.99
Cathepsin D OS=Cricetulus griseus OX=10029 GN=H671_3g9701 PE=3 SV=1	1.18E+05	0.002	44.1	6.98
Glutathione synthetase OS=Cricetulus griseus OX=10029 GN=I79_007504 PE=3 SV=1	1.10E+05	0.002	52.2	5.57
Leukocyte elastase inhibitor A OS=Cricetulus griseus OX=10029 GN=CgPICR_009798 PE=3 SV=1	1.09E+05	0.002	42.9	6.16
Vimentin OS=Homo sapiens OX=9606 GN=VIM PE=1 SV=4	1.06E+05	0.002	53.6	5.12
Activated RNA polymerase II transcriptional coactivator p15 OS=Homo sapiens OX=9606 GN=SUB1 PE=1 SV=3	1.05E+05	0.002	14.4	9.6
Collagen alpha-1(V) chain OS=Homo sapiens OX=9606 GN=COL5A1 PE=1 SV=3	1.03E+05	0.001	183.4	5.06
Prelamin-A/C OS=Homo sapiens OX=9606 GN=LMNA PE=1 SV=1	1.01E+05	0.001	74.1	7.02
ARHGDI1 OS=Cricetulus griseus OX=10029 GN=CgPICR_011939 PE=4 SV=1	1.01E+05	0.001	23.4	5.2
Golgi apparatus protein 1 OS=Homo sapiens OX=9606 GN=GLG1 PE=1 SV=2	9.96E+04	0.001	134.5	6.9
Heat shock protein HSP 90-alpha OS=Homo sapiens OX=9606 GN=HSP90AA1 PE=1 SV=5	9.60E+04	0.001	84.6	5.02
Mpv17-like protein 2 OS=Cricetulus griseus OX=10029 GN=I79_005109 PE=4 SV=1	8.85E+04	0.001	52.4	8.24
Acid ceramidase OS=Cricetulus griseus OX=10029 GN=I79_003173 PE=3 SV=1	8.07E+04	0.001	44.7	7.9
Heat shock cognate 71 kDa protein OS=Homo sapiens OX=9606 GN=HSPA8 PE=1 SV=1	7.64E+04	0.001	68.8	5.52
Collagen alpha-2(V) chain OS=Cricetulus griseus OX=10029 GN=I79_024376 PE=4 SV=1	7.48E+04	0.001	19	7.72
Nucleophosmin OS=Cricetulus griseus OX=10029 GN=I79_020971 PE=4 SV=1	7.01E+04	0.001	31	4.67
Neuroplastin OS=Homo sapiens OX=9606 GN=NPTN PE=1 SV=2	6.65E+04	0.001	44.4	7.99
ARSA OS=Cricetulus griseus OX=10029 GN=CgPICR_000077 PE=4 SV=1	6.38E+04	0.001	55	5.15
Nucleoside diphosphate kinase A OS=Homo sapiens OX=9606 GN=NME1 PE=1 SV=1	6.29E+04	0.001	17.1	6.19
Di-N-acetylchitinase OS=Cricetulus griseus OX=10029 GN=I79_011948 PE=3 SV=1	6.19E+04	0.001	32.9	5.67
Matrix metalloproteinase-9 OS=Cricetulus griseus OX=10029 GN=I79_006812 PE=3 SV=1	5.65E+04	0.001	78.8	5.94
Lactotransferrin (Fragment) OS=Homo sapiens OX=9606 GN=LTF PE=1 SV=1	5.55E+04	0.001	76.6	8.02
Chondroitin sulfate proteoglycan 4 OS=Cricetulus griseus OX=10029 GN=I79_003599 PE=4 SV=1	5.05E+04	0.001	251.9	5.68

Neogenin OS=Cricetulus griseus OX=10029 GN=I79_008978 PE=4 SV=1	4.94E+04	0.001	154.4	6.64
Serine/threonine-protein kinase DCLK2 OS=Cricetulus griseus OX=10029 GN=I79_011199 PE=4 SV=1	4.68E+04	0.001	108.3	6.81
Transaldolase OS=Cricetulus griseus OX=10029 GN=I79_024784 PE=3 SV=1	4.39E+04	0.001	36.1	5.24
Pantetheinase OS=Cricetulus griseus OX=10029 GN=I79_019325 PE=4 SV=1	4.32E+04	0.001	56.7	5.63
Protein S100 OS=Cricetulus griseus OX=10029 GN=H671_1g3381 PE=3 SV=1	4.24E+04	0.001	11.2	7.08
N-sulphoglucosamine sulphohydrolase OS=Cricetulus griseus OX=10029 GN=CgPICR_011967 PE=4 SV=1	4.21E+04	0.001	56.5	6.52
Deoxyuridine 5'-triphosphate nucleotidohydrolase, mitochondrial OS=Homo sapiens OX=9606 GN=DUT PE=1 SV=1	3.67E+04	0.001	15.4	6.57

Note: analysis of rhGNS from myc affinity purification from TCB616 C2 by LC/MS/MS analysis determined no major contaminant proteins from CHO cells.

Supplemental Methods

1. Assay Optimization GNS Assay

While the Sulfatase Assay provided a direct measurement of sulfatase activity, it is worth noting that para-nitrocatechol sulfate (PNCS) is a common substrate of several sulfatases and therefore lacks substrate specificity. To address this, we utilized a coupled, fluorometric assay using 4-MU-GNS, which has been used previously and more closely mimics the natural substrate of the GNS enzyme, which we term the “GNS Assay”. The GNS activity assay was completed in two parts, where the first step involved incubation with 4-MUGNS, producing 4-methylumbelliferyl-2-acetamido-2-deoxy- α -D-glucopyranoside, and the second step involved addition of α -N-acetylglucosaminidase (NAGLU) to release 4-MU, which exhibits an excitation/emission profile of 360/450nm. The GNS assay was first developed over twenty years ago primarily for the diagnosis of MPSIIID patients; therefore the assay was carried out over a prolonged 24-48 hour incubation period due to the low concentration of the enzyme present in cell lysates of healthy individuals.

Because the assay requires two sequential reaction steps, it was essential that the second step enzyme was not limiting for the amount of product produced from the first (GNS) reaction. Therefore, highly concentrated stocks of recombinant human NAGLU conditioned media were produced. We then used this concentrated media for optimization and found that using 5 μ L of the 20 x concentrated rhNAGLU stock after 30 minutes we were able to achieve complete turnover of 4-methylumbelliferyl-2-acetamido-2-deoxy- α -D-glucopyranoside produced by 20 ng of rhGNS after one hour reaction time (>250 nmol 4-MU).

2. Sulfatase Assay

An absorbance-based measurement of GNS sulfatase activity was adapted from the protocol provided by R&D systems with modifications using a 96-well plate format. Each well containing 10 μ L of 2 μ g/mL rhGNS in reaction buffer 1 (200 mM sodium acetate, pH 5.6, 0.01% Triton X-100) was incubated with 40 μ L of 2.5 mM para-nitrocatechol sulfate (PNCS) for 1-4 hours at 37 °C. Following incubation, 50 μ L of 0.2 M NaOH was added to stop reactions, and plates were then centrifuged at 1000 rpm for 1 min. Absorbance was measured at 510 nm using the Synergy Neo 2 Multi-Mode microplate reader (BioTek). Each reaction condition was carried out in triplicate.

3. Assay Optimization Sulfatase Assay

Two assays were used to assess GNS activity, the first of which is a colorimetric assay utilized para-nitrocatechol-sulfate (PNCS), an artificial substrate of non-specific sulfatase activity. Cleavage of the sulfate group occurs in a one-step reaction producing para-nitrocatechol (PNC), yielding maximum absorbance at 510 nm under basic conditions and referred to as the “Sulfatase Assay”. Individual buffer components were optimized in independent experiments. Enzyme activity remained relatively stable up to levels of 250 mM NaCl, whereas acetate concentration showed very minor effects. Experiments with other common biological buffers demonstrated that the enzyme is completely inhibited in the presence of free phosphate, sulfate, or citrate groups. Therefore, purification and other assay buffer conditions were similarly optimized to avoid addition of these components. Addition of the detergent Triton X-100 (Sigma) significantly increased reproducibility and showed maximal enzyme specific activity at low concentrations (0.01%). In order to test activity over a range of pH, we use three buffer conditions to cover the range of pH values: acetate (pKa=4.76; range=3.2-5.6), MES (pKa=6.16; range=5.5-6.7), and HEPES (pKa=7.55; range=6.8-8.2).

4. SDS-PAGE and Western Blotting

Samples were loaded on a 4-20% Tris-Glycine Mini-PROTEAN Gels (Bio-Rad) along with Kaleidoscope™ protein standard (Bio-Rad) as a molecular weight marker. Protein bands were visualized by staining with Imperial™ protein stain (Thermo Scientific, Waltham, MA) or transferred onto nitrocellulose membranes using the Trans-Blot Turbo system (Bio-Rad) for western blotting. After blocking with 5% milk in TBST (20 mM Tris, 150 mM NaCl, 0.1% (w/v) Tween-20), membranes were probed with either goat anti-GNS antibody (R&D Systems, AF2484), mouse anti-c-myc antibody (Thermo Scientific, Waltham, MA1-21316), mouse anti-LAMP1 (DSHB, 1D4B), or rabbit anti-GAPDH (CST, Cat # 2118) overnight at 4 °C. After washing, membranes were incubated for 2 hours at room temperature with HRP-conjugated secondary antibodies. ECL reagent (WBKLS0500, MilliporeSigma) and ChemiDoc MP Imaging System (Bio-Rad) were used to image the blots. Gel bands quantification was performed using Image J.

5. Native Polyacrylamide Gel Electrophoresis

Native polyacrylamide gel electrophoresis was performed using Novex Tris-Glycine Gels (Cat# XP00100BOX, ThermoFisher). Purified rhGNS was mixed with Novex Tris-Glycine Native Sample Buffer (Cat# LC2673, ThermoFisher), 0.5 µg protein was loaded into each lane. Run the gel at 225 V constant for 35 minutes.

6. Thermal Shift Assay

Thermal shift assay was performed with Tycho (Nanotemper, Germany), utilizing intrinsic tryptophan fluorescence. Generally, purified rhGNS was diluted in artificial CSF to 10 µg/mL, then centrifuge for 30 minutes at 13,000 g, 4 °C. Clean capillary (Tycho NT.6 Capillaries, Nanotemper) was filled with supernatant then loaded into capillary tray. Samples were heated from 35 °C to 95 °C in 3 minutes and inflection temperature was calculated by the software automatically.

7. Lysosome Purification

The lysosome fractions from brains harvested from MPS IIID mutant (GNS^{-/-}) mice treated with or without rhGNS along with age-matched carrier control (GNS^{-/-}) mice were enriched using the Lysosome Enrichment Kit for Tissue and Cultured Cells (Thermo Scientific, Waltham, MA) according to the manufacturer's instructions. Isolated lysosomes were lysed in GNS lysis buffer before enzyme activity assays and Western blots.

8. LC/MS/MS

In solution tryptic digest followed by nano-liquid chromatography–tandem mass spectrometry analysis. Purified protein (100 µL) were diluted with 25 µL 100 mM Tris buffer (pH 8.5), reduced with 1 µL 0.5 M tris (2-carboxyethyl) phosphine hydrochloride (Thermo Fisher Scientific) for 20 min at 37 °C, alkylated with 3 µL 0.5 M chloroacetamide (Fisher) for 15 min at 37 °C, and digested with 2 µL 100 ng/µL Lysyl endopeptidase (Wako Chemicals; Lys-C) for 4 h at 37 °C. And then digested with 3 µL 100 ng/µL trypsin (Thermo Fisher Scientific) with 5 µL 100mM CaCl₂ for 18 h at 37 °C. After desalting with Pierce C18 Tip (Thermo Fisher Scientific), peptides were eluted with 200 µL 75% (vol/vol) acetonitrile (ACN) 0.1% TFA. Solvent was removed using a SpeedVac.

For rhGNS purified from TCB469 B2 (table S4), dried peptides were acidified by 0.2% formic acid and loaded onto an Easy Nano-LC Q-Exactive Orbitrap (Thermo Fisher Scientific). Peptides were loaded onto a trap column [PepMap 100 C18, 3 μm , 75 μm \AA x 2 cm, nanoViper (Thermo Fisher Scientific)] and separated with an Easy-Spray column [PepMap C18, 3 μm 100 \AA , 75 μm \AA x 15 cm (Thermo Fisher Scientific, ES800) with a 2–30% (vol/vol) gradient (A: 0.1% formic acid [FA] in water; B: 0.1% FA in 100% CAN)] at 300 nL/min for 60 min followed by 30% (vol/vol) B to 100% B for 5 min and incubated at 100%B for 10 min. The Q-Exactive acquisition method was created in data-dependent mode with one precursor scan in the Orbitrap, followed by fragmentation of the 15 most abundant peaks. Resolution of the precursor scan was set to 70,000, automatic gain control target 3e6, maximum injection time 100 ms, scanning from 350 to 2,000 m/z. The MS2 resolution was 17,500, the AGC target 5e4, the isolation window was 2.0 m/z, the fixed first mass 100.0 m/z, the normalized collision energy was 25, the underfill ratio was 0.1%, the charge exclusion was unassigned 1, peptide match was preferred, the exclude isotope option was on, and the dynamic exclusion was 30.0 s. The peak list generating software used was Proteome Discoverer Software (Thermo Fisher Scientific). The outline of the method used in the spectrum selector mode of the Proteome Discoverer software were all set to default settings to generate tandem MS spectra. The precursor charge state (high/low), retention time, minimum peak count, and total intensity threshold value were all set to default settings. The maximum and minimum precursor mass settings were 5,000 and 350 Da, respectively. The Human Fasta file (canonical and isoform) was downloaded from UniProt (www.uniprot.org).

The Sequest HT search parameters included in this study were two missed cleavages allowed, fully tryptic peptides only, minimum peptide length of 6, maximum peptide length of 144, fixed modification of carbamidomethyl cysteine (+57.021 Da), dynamic modifications of oxidized methionine (+15.995Da), and N-terminal acetylation (+42.011Da). The precursor ion mass tolerance was 10 ppm and fragment mass tolerance was 0.05 Da. The input data maximum delta was Cn 0.05. The decoy database search was applied with strict false discovery rates (FDR) of 0.01 and relaxed FDR of 0.05, where the validation was based on q value.

For rhGNS purified from TCB616 C2, dried peptides were acidified by 0.2% formic acid and subjected to LC-MS/MS analysis on an EASY-nLC 1200 coupled to a Q Exactive HF Orbitrap mass spectrometer (Thermo Fisher Scientific, Bremen, Germany) equipped with a Nanospray Flex ion source. Peptides were directly loaded onto an Aurora 25cm x 75 μm ID, 1.6 μm C18 column (Ion Opticks) heated to 50°C. The peptides were separated at a flow rate of 350 nL/min with the following gradient: 2–6% Solvent B (2 min), 6–25% B (20.5 min), 25–40% B (7.5 min), 40–98% B (1 min), and held at 98% B (12 min). Solvent A consisted of 97.8 % H₂O, 2% ACN, and 0.2% formic acid and solvent B consisted of 19.8% H₂O, 80 % ACN, and 0.2% formic acid. Full scan resolution was set to 60,000 at m/z 200. Full scan target was 3e6 with a maximum injection time of 15 ms. Mass range was set to 375–1500 m/z. For data dependent MS2 scans the loop count was 12, minimum AGC target value was set at 4.5e3, intensity threshold was 1e5, and maximum injection time was 45 ms. Isolation width was set at 1.2 m/z and a fixed first mass of 100 was used. Normalized collision energy was set at 28. Peptide match was set to off and isotope exclusion was on. MS2 scans were acquired in centroid mode at a resolution of 30,000.

Raw data were searched in Proteome Discoverer 2.4 (Thermo Scientific) using the Byonic search algorithm (Protein Metrics) and a FASTA file containing all human and Chinese hamster Uniprot protein sequences as well as common contaminants. PD-Byonic search parameters were as follows: fully

Tryptic peptides with no more than 2 missed cleavages, precursor mass tolerance of 10 ppm, fragment mass tolerance of 20 ppm, and a maximum of 2 common modifications and 2 rare modifications. Cysteine carbamidomethylation was set as a static modification, while methionine oxidation was a common dynamic modification (up to 2 per peptide). Methionine loss on protein N-termini, methionine loss + acetylation on protein N-termini, protein N-terminal acetylation, and lysine acetylation were rare dynamic modifications (only 1 each). Byonic protein-level FDR was set at 0.01, while Percolator FDRs were set at 0.01 (strict) and 0.05 (relaxed). In the consensus step, peptide and PSM FDRs were set at 0.001 (strict) and 0.01 (relaxed), with peptide confidence at least medium, lower confidence peptides excluded, minimum peptide length set at 6, and apply strict parsimony set to false. Quantified peptides included unique + razor, protein groups were considered for peptide uniqueness, shared Quan results were not used, and Quan results with missing values were not rejected. Precursor abundances were determined based on intensity, and the protein abundances were calculated as the sum of each protein's peptide group abundances. The protein abundances were then used to estimate purity of the GNS prep, with the GNS abundance set at 100% and all other proteins normalized to this.